Measurement of the Energy-Dependent Angular Response of the ARES Detector System and Application to Aerial Imaging

Tenzing H. Joshi, Jonathan Maltz, Mark Bandstra, Brian J. Quiter

Lawrence Berkeley National Laboratory, Berkeley, CA 94720 USA

Eric Wagner, Tanushree Luke, Russell Malchow, Karen McCall

Remote Sensing Laboratory, Las Vegas, NV 89193, USA

ABSTRACT

The Airborne Radiological Enhanced-sensor System (ARES) system includes a prototype helicopter-borne CsI(Na) detector array that has been developed as part of a DHS Domestic Nuclear Detection Office Advanced Technology Demonstration. The detector system geometry comprises two pairs of 23 detector arrays designed to function as active masks, providing additional angular resolution of measured gamma rays in the roll dimension. Experimental measurements, using five radioisotopes (^{137}Cs, ^{60}Co, ^{241}Am, ^{131}I, ^{99m}Tc), were performed to map the detector response in both roll (θ) and pitch (ϕ) dimensions. This work describes the acquisition and analysis of these characterization measurements, calculation of the angular response of the system, and how this response function is being used to improve aerial detection and localization of radiological and nuclear sources.

EXPERIMENTAL CHARACTERIZATION OF THE ARES DETECTOR SYSTEM

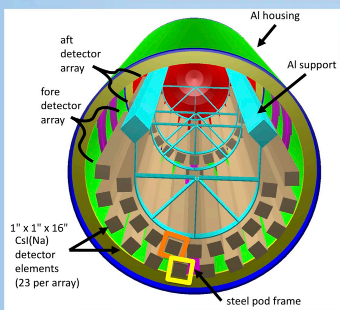

Schematic end-on view of one ARES pod. Each pod contains two 23-detector arrays arranged to provide angular resolution in the roll dimension. Detectors 55, 56 are indicated in orange and yellow respectively.

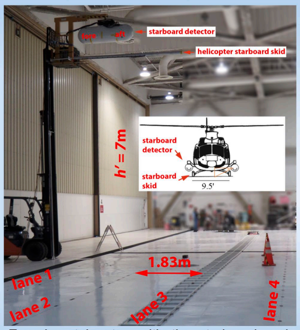

Experimental setup with the starboard pod. Sources were moved along lanes 1-6 to characterize the detector response as a function of roll, pitch, and gamma-ray energy.

Calibration Sources Used		
Isotope	Activity (mCi) at t_0	Energy (keV)
^{241}Am	5.4	59
^{99m}Tc	20.1	140
^{131}I	7.9	364
^{137}Cs	3.2	662
^{60}Co	2.9	1173, 1332

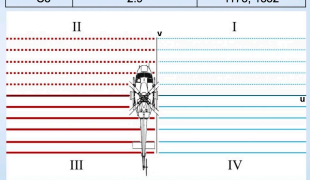

Schematic of the phase space mapped with measurements. Quadrants III and IV were mapped out for the starboard pod, the six lanes used for measurements are indicated in solid. Symmetry was used to calculate the response for the quadrants I and II and for the port pod.

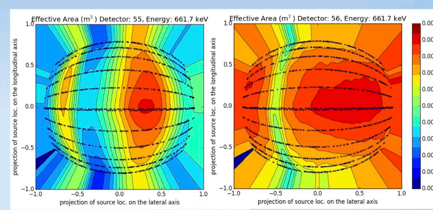

Experimentally derived angular response of the two detectors (55,56). These plots show the sensitivity of each detector, in units of effective area (color), as a function of the source direction projected on the lateral/roll axis (abscissa) and longitudinal/pitch axis (ordinate). Points illustrate a subset of locations where measurements were made. Interpolation and smoothing filters were then applied to results prior to plotting. Detector 55 exhibits the narrow angular response of detectors from the inner positions, while detector 56 illustrates the broad angular response of detectors at outer positions, but with a feature corresponding to the helicopter skid.

DISTRIBUTED SOURCE (^{40}K)

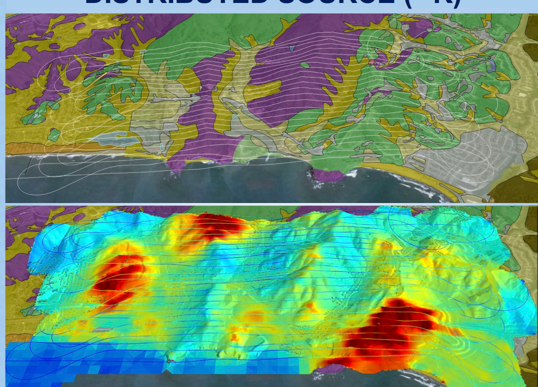

(top) Helicopter flight path over Pacifica, California with terrain colored by USGS geologic material map. Mountainous terrain and varying geology make this region an excellent proving ground for aerial measurement systems. The flight path covered a 4.5x2.5 km area. (bottom) Sensitivity-corrected back-projection (color) of measurements of the 1460 keV gamma-ray from ^{40}K overlaid on satellite imagery. Flight path is colorized by 1460 keV rate in the entire detector system. Imaging pixels come from a topographic database with approximately 10 m^2 pixels.

POINT SOURCE (^{137}Cs)

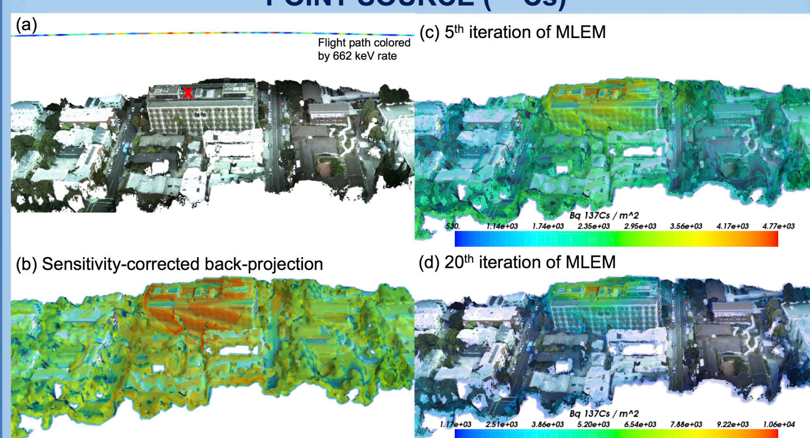

Demonstration of point source localization using 7.8 seconds of flight data. During data collection, a 1.5 mCi ^{137}Cs source was placed on the roof of Etcheverry Hall, red X in figure (a). The spatial scene and time-dependent helicopter pose, (a), was reconstructed via simultaneous localization and mapping (SLAM) using time-synchronized helicopter imagery, the helicopter path is colored by 662 keV event rate. The spatial scene was segmented with 2 m length voxels then used for image reconstruction.

METHODS

The energy dependent angular response (photo-peak efficiency) of each detector, η(E,*d,θ,ϕ)*, was calculated as:

$$\eta(d,E,\theta,\phi)=\frac{4\pi r_{ds}^2\left(\frac{s(d,E,\theta,\phi)}{\Delta t_s}-\frac{b(d,E)}{\Delta t_b}\right)}{A(E,t_0)BR(E)e^{-t/\tau}e^{-\mu_{air}(E)r_{ds}}}$$

$$t=f(\theta,\phi),\ r_{ds}=f(\theta,\phi)$$

Background subtracted photopeak rate is scaled by the attenuated gamma-ray flux.

For radiological mapping, spatial context and helicopter pose were acquired via two methods:
1) a terrain database and GPS/INS data
2) simultaneous localization and mapping (SLAM) using visual imagery.

Photo-peak rate at a particular pose:

$$C(d,E)=\sum_i \frac{\eta(d,E,\theta_i,\phi_i)}{4\pi r_{di}^2 e^{\mu_{air}r_{di}}}\frac{\cos(\omega_{di})}{\mu_i}A_i(E)$$

Combining many measurements, from many detectors and poses:

$$\begin{bmatrix} C_0 \\ C_1 \\ \vdots \\ C_n \end{bmatrix}=\begin{bmatrix} P_{0,0} & P_{0,1} & \dots & P_{0,m} \\ P_{1,0} & P_{1,1} & \dots & P_{1,m} \\ \vdots & \vdots & \vdots & \vdots \\ P_{n,0} & P_{n,1} & \dots & P_{n,m} \end{bmatrix}\begin{bmatrix} A_0 \\ A_1 \\ \vdots \\ A_m \end{bmatrix}$$

Sensitivity-corrected back-projection

$$\frac{P^T C}{P^T \mathbf{1}}$$

MLEM

$$A^{k+1}=\frac{A^k}{P^T\mathbf{1}}P^T\frac{C}{PA^k}$$

ARES IN ACTION

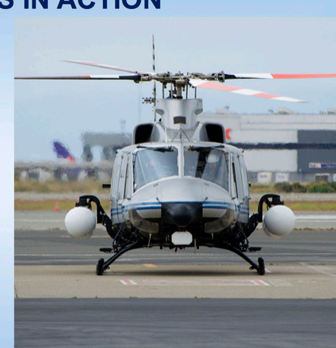

ACKNOWLEDGEMENTS

We would like to thank Andrew Haefner for producing the 3D scene from the Etcheverry flight data, Andrew Haefner and Donald Gunter for many insightful conversations, and Mark Bandstra and Victor Negut for the ARES photography. This work has been supported by the US Department of Homeland Security, Domestic Nuclear Detection Office, under IAA HSHQDC-11-X-00380. This support does not constitute an express or implied endorsement on the part of the Government. A portion of this work was performed by National Security Technologies, LLC, under Contract No. DE-AC52-06NA25946 with the U.S. Department of Energy. DOE/NV/25946--2714